

11th International Symposium on Rock Fragmentation by Blasting

Paper Number: 2.00

Time Correlated Response of Multi-Story, Urban Structures to High Frequency Blasting Excitation

C Dowding¹, C Aimone-Martin² and P Abeel³

1.
Professor, Civil & Environmental Engineering, Northwestern University, Evanston, IL 60208. Email: c-dowding@northwestern.edu
2.
President, Aimone-Martin Associates, 1005 Bullock Boulevard, Socorro, NM 87801. Email: cathy@aimonemartin.com
3.
Engineer, Subsea 7, 17220 Katy Freeway Suite 100, Houston, TX 77094. Email: abeel.pa@gmail.com

ABSTRACT

This paper presents measurement and analysis of the dynamic response of a five-story building to very-high frequency excitation (> 100 Hz) from blasting vibrations originating from a contiguous excavation of rock. Velocity response measurements, in the rock and on the structure, were employed to calculate time correlated dynamic displacement response of the building to blasting. Time correlated structure response measurements are needed to advance the understanding of the response of urban structures to high frequency excitation. Current regulations and understanding are based upon measurements of the response of one to two story residential structures by 10 to 40 Hz excitation. Extension of these observations to taller structures when excited by high frequency excitation needs to be investigated further.

Measurements show that the amplification patterns at the ground level and top of the structure match or are lower than that observed by the US Bureau of Mines (Siskind, et al., 1980) for the shorter residential structures. They decrease with increasing peak particle velocity. From the measurements, the global transverse shear strains found by differentiating ground floor and top displacements were calculated to be 12 μ strains. Time correlated bottom and top of structure displacements show that building response may be more reflective of wave propagation up the structure than whole-structure inter story drift.

In addition a 3D model was used to compare computed displacements and strains to measured results. Modeled responses varied considerably both in magnitude and location of the maximum strain. No conclusion can be made regarding the best 3D model to employ to simulate building response. More data such as motions measured at many points in the structure are needed. Maximum inter-story transverse shear strains calculated with the model were found through the acceleration excitation and were less than 12 μ strains for 37 mm/s rock motion excitation. The inter-story transverse shear strains calculated with rock displacement input were less than that found with the acceleration excitation.

INTRODUCTION

This paper presents measurement and analysis of the dynamic response of a five-story building to very-high frequency excitation (> 100 Hz) from blasting vibrations originating from a contiguous excavation of rock. Velocity response measurements, in the rock and on the structure, were employed to calculate time correlated dynamic displacement response of the building to blasting. Time correlated structure response measurements are needed to advance the understanding of the response of urban structures to high frequency excitation. Current regulations and understanding are based upon measurements of the response of one to two story residential structures by 10 to 40 Hz excitation. Extension of these observations to taller structures when excited by high frequency excitation needs to be investigated further. This paper presents measured and modeled responses necessary to begin this investigation. It addresses such questions as; how do such structures respond to close in blasting? Are the responses synchronous? What are likely strain levels?

Site and Blast Vibration Environment

The five-story test structure was constructed in the early 1900s. It is a masonry load bearing structure with a three-wythe exterior brick wall. Its dimensions are 7m [W] x 19.5m [L] x 19.8m [H]. Figure 1 is a photograph of the building and the immediately adjacent rock. The lower back building on the left is not attached to the instrumented structure.

The adjacent excavation shown in Figure 1 is approximately 24m by 60m. Excavated rock was predominately metamorphic schist. While variable from shot to shot, a typical blast consisted of approximately 10 to 20 holes arranged in two rows with an 2.5x2.5 m pattern or S/B = 1. Each hole was detonated separately with two to four kg of explosive per hole. Blasting progressed west to east from south to north, which means that the source location of the blast differed for every detonation. Thus each blast occurred at different distance and angle to the building and fixed instrument locations. Unfortunately, exact blast locations were unknown.

Instrumentation

In-rock instrumentation was located at several positions to account for the progressive advance of the blasting. Before every shot, a three-component geophone was inserted in a drilled hole close to the blasting area and adjacent to the structure as shown in Figure 1. These in-rock geophones were designed to be reused and could be moved during excavation. Measurement point seven (MP7) was placed first before the structure instrumentation started, as blasting began in the tight northwestern corner south of the building.

As shown in Figure 1, the structure was instrumented with two sets of geophones on the East wall. Each set was composed of two transducers to measure the horizontal radial and transverse building response. One set was bolted on the ground floor at the street level, while the other was bolted to the base

of the roof parapet directly vertical above the street level set. Ground/street level is one floor above the rock-building interface. These geophones meet the ISEE standards with -3 dB velocity response between two and 256 Hz.

MEASURED RESULTS

During the observation period, nine blasting events in Table 1 were monitored. Time histories are preserved in Abeel (2012). A typical suite of vibration records is presented in Figure 2, for both transverse and longitudinal directions (or perpendicular and parallel to the rear wall). Comparison of these high frequency excitation time histories in Figure 2 and Table 1 describes a variety of phenomena. Dominant frequencies of these motions decline from the in-rock excitation (higher than 150Hz) to the structure response of 7Hz to 40Hz. Amplitude of the motion at either the top or street/ground level declines or increases only slightly when compared to those measured in the rock.

Such data comparing close-in rock excitation with building response are relatively rare. In rural areas, small distances between blast and structure are rare. In urban areas, adjacent excavations often preclude measurement of the motions in the rock itself. Thus compliance transducers are often placed on the structure at its lowest accessible floor. As the excavation deepens, this ground level or basement transducers become less and less equivalent to the excitation location.

Transducer location details can affect measured response. For instance, in this study “ground level” transducers were placed on the outside of the building without exact knowledge of the interior shear wall locations. Therefore, ground level measurements may be recording a mixture of by wall and superstructure motions. Top transducers were attached to the lowest portion of the parapet to avoid penetrating roof waterproofing membrane. Therefore, they too may be responding to a mixture of parapet and superstructure motions as well.

Low Frequency Riders on Velocity and Displacement Time Histories

Comparison of in-rock and building response from this study shed some light on the low frequency rider on high-frequency velocity measurement such as that in the ground level radial recording shown in Figure 2. The low frequency rider can be seen at the end of the unfiltered, ground level, radial motions in the middle right time history. Several reasons have been advanced for such low frequency riders:

- actual displacements from poorly attached velocity transducers
- delayed gas pressure excitation
- velocity transducer response itself

Considering this case, the ground level transducers were bolted to the structure and are unlikely to have been displaced permanently. In-rock transducers, the most likely to be subjected to delayed gas pressure, show no such response. Furthermore, only the motions parallel to the building (radial) not perpendicular (transverse) display the low frequency rider. Thus in this case it appears that the most likely reason is the high frequency transducer response itself. While personal discussions with instrument manufacturers (Wheeler R., 2012; Turnbull R., 2012) showed that they have been able to reproduce these responses in the laboratory, the investigation of this phenomenon is continuing.

Estimation of Natural Frequency and Damping Response of Structure

If the building is idealized as a single degree of freedom (SDOF) system, its response characteristics can be reduced to its natural frequency, f , and its damping ratio, β . Values of f and β can be found using a Fourier frequency transfer function (FFT) (Dowding, 1996) equal to the ratio of the FFT of the time history at the top of the structure divided by the FFT at the ground level. The values obtained, $f = 7.5\text{Hz}$ and $\beta = 3.2\%$, are compatible with values previously documented (Dowding, 1996) and will be used as inputs in the SDOF model presented later. These calculations can also be compared with the free response of the building as shown in Figure 2.

Ratios of Response to Excitation

Ratios or response to excitation peak particle velocity (PPV) in Table 1 when plotted against rock excitation PPV's in Figure 3 show that building response is deamplified (declines below 1) at high PPV rock excitation. Ratios were computed using peak values at each level, and not time-correlated values. Thus they are conservative. Time correlated values will be lower (Essaib, 2015). Comparisons focus on the transverse direction, which describes the out-of-plane displacements. Not only is the building narrower in this direction, thus presenting a lower structure stiffness, but it is also the direction of the highest wall responses. Declination is most likely the result of the increased dominant excitation frequency of the rock as the blasts

approach the building and produce a larger rock PPV. Since the blasts were designed with similar charge weights with delay; the higher the rock PPV, the smaller the distance to the structure.

3D MODEL OF THE DISPLACEMENT AND STRAIN RESPONSE OF THE STRUCTURE

Model-ware, Parameters, and Inputs

The 3D model (SAP 2000) shown in Figure 4 was employed to determine if “in-rock” excitation motions could be used to estimate or predict building response. Ability to simulate response with this model is assessed by comparing various approaches to calculate building displacements with those measured. Table 2 presents the building parameters employed in the model. Values were chosen because they were reasonable and typical. The model was not modified to fit the measured response. The contact nodes located at the base of the structure columns were modeled as fixed constraints. Model response can either be deformation, displacement or stress at any point of the structure. Displacements of the nodes corresponding to the location of the instrumentation (along line A at level “2” and “top” in Figure 4) were compared to those measured.

Variation of Input Employed with the Model

Excitation motions used to perturb the model can either be an acceleration time history or boundary displacement motions applied to every node in contact with the ground. In the case of an acceleration input, a sample acceleration time history can be used to simulate any kind of vibration such as an earthquake or, in the case of this study, a blast. This excitation will however be the same across the whole structure, thus it cannot account for the attenuation and change in phase that occurs as the excitation vibration waves propagate through the rock.

Excitation by boundary node displacement allows more factors to be taken into account. As the waves propagate away from the source of the blast with a defined propagation velocity, the amplitude should attenuate with distance, as is often observed. As this distance between blast and excitation node increases, the amplitude should decline. In addition, differences in travel distances between blast and excitation node result in differences in arrival times. Differences in arrival time can be calculated by dividing the different travel distances by the propagation velocity, which were estimated to be 2743 m/s in the rock (Hamdi, 2015).

SAP 2000 software allows the user to account for the attenuation and time delay by employing displacements of the ground nodes as an input. A different displacement time history for each bottom node can be specified at each point. Displacements were obtained by integrating the “in-rock” excitation particle velocity time histories. Three cases were computed with this displacement input:

- 1) & 2) Non-attenuated, non- time delayed displacement input, where only one displacement and one acceleration time history is employed. An example of a typical set of time histories for this non delayed input is shown in Figure 5, with acceleration, velocity, and displacements plots. The event acceleration time history was established by differentiating the velocity time history and the displacement time history was produced by integrating the velocity time history. This displacement time history is then used as an input to the model on every ground node, without any attenuation or delay. This approach is similar to techniques employed in earthquake structural dynamics where the wave lengths are much longer than the structure’s footprint.
- 3) An attenuated and time delayed displacement input that varies at each node, where the arrival time is listed in Table 3 for each foundation node. The delay between diagonal corners is some 7.5 ms with a propagation velocity of 2743 m/s. The attenuation was estimated to be 60% along the structure given a travel distance of some two wave lengths of a 250 Hz wave.

Finally, a fourth model can be used to compute the expected deformation of the structure: idealization as a single degree of freedom system (SDOF). Values of the SDOF natural frequency f and the damping ratio β obtained from the transfer function are used as building parameters: $f_s = 7.5\text{Hz}$ and $\beta = 3.4\%$. These values can be compared to the ones that were automatically computed by SAP 2000 from the structural parameters that were entered: $f_s = 7.6\text{Hz}$ with an assumed damping ratio of 5%. The SDOF model compacts all geometry, mass, stiffness and damping into two parameters, f_s and β .

Response of these four models (three multiple-degree-of-freedom models and one single-degree-of-freedom) can be compared to the measured displacements at the top of the structure, as shown in Figure 6. It appears that the results given by the acceleration excitation (top) correlate best with those measured (bottom). This correlation is better than that of either of the displacement input models. All of the multi-degree of freedom response correlated better than that of the SDOF response.

Strain Calculation and Representation

Inter-story shear strains acting on the inside transverse shear walls were calculated along the vertical line A in Figure 4 from the computed displacements. Figure 7 illustrates the method used to compute these shear strains, while Figure 8 compares them to the global shear strain computed from the measured displacements. They were found by differentiating ground floor and top displacements, as shown in Figure 7, and were calculated to be 11.4 micro-strains, which is low compared to an applicable threshold for the potential of hair line or cosmetic cracking.

Hair line, cosmetic cracking potential can be based on failure strains as reported by Aimone & Meins (2014) and summarized as follows. Siskind (2000) reports that visible surface cracks were observed in the weakest materials found in buildings: 300 μ -strains in drywall plaster core and aged mortar (the onset of visible mortar cracks appeared at 470 μ -strains). No information is available in the U.S. literature on nonmilitary dynamic testing providing failure strains for lime and gypsum plasters typically used as wall coating in historic and older structures. Laboratory testing of typical Brazilian cement grout samples made with varying cement, lime, and water ratios and used for surface wall coating is reported by Rosenhaim et al., (2014). Diametral and beam bending test results show failure strains range from 153 to 286 μ -strains. Therefore, a conservative threshold of 100 to 200 μ -strains can be employed as an indication of possible hairline cracking in historic plaster.

Inter-story shear strains in Figures 7 & 8 were found from the peak displacement pulse produced by the acceleration perturbation shown on the right middle of Figure 7. These were the computed displacements on the south-east corner (vertical line A). They were determined at the same instant of time during the pulse at 0.66s. The strain distribution along vertical lines A, B and C are compared in the figure on the lower right. This procedure was also followed at 0.645s and the two strain distributions are elsewhere (Hamdi, 2015). Figure 9 presents a calculation of the propagation velocity in the structure as a function of the time delay between the measured displacement time histories at the top and the ground level. The propagation velocity of the wave in the structure was calculated to be 1,050 m/s. This lag would not be observed in one to two story residential structures investigated by Siskind et al (1980).

DISCUSSION AND CONCLUSIONS

Presented in this paper is analysis of measured dynamic response of a five-story building to ultra-high frequency blast vibration excitation from contiguous rock excavation. Velocity time histories recorded in the rock and on the structure are integrated to calculate dynamic displacement response of the building to blasting. A 3D model is used to compare simulated displacements and strains to those calculated from measured velocity time histories.

Even though responses were measured only along one vertical line and thus do not fully describe the variety of response of the entire structure, they do represent several steps forward in instrumentation in urban environments. Velocity time histories were measured “in-rock” as well as on the building. Those on structure at the “ground floor” level and at the top were time correlated to allow calculation of strain from inter-story differential displacement or (drift). These atypical measurements allowed comparison of “true” rock excitation motions to response motions and building strains calculated from differences in inter-story displacement drift. These measurements allow the advancement of the following observations:

- Peak particle velocity (PPV) building response declines to less than excitation rock PPV with increasing rock excitation PPV.
- Global transverse shear strains found by differentiating ground floor and top displacements were calculated to be 12 micro-strains. These strains are low and below those that might cause cosmetic cracking.
- Time histories of building response displayed wave propagation induced delays and do not demonstrate synchronous response associated with the response of one to two story residential structures
- Models employed to simulate time histories of structural response returned a range of amplitudes and require more study.
- Maximum inter-story transverse shear strains in the modeled structure were found through uniform acceleration excitation and were less than 12 μ strains for a 37 mm/s (1.5ips) rock motion, and declined with elevation. Inter-story transverse shear strains calculated with uniform rock displacement excitation were 65% of that found with the uniform acceleration excitation.

ACKNOWLEDGEMENTS

This article could not have been written without the cooperation of the building developer, blasting subcontractor, neighbouring property owners and regulatory authorities. However in this case the identity of these individuals and organizations are best served if they remain unknown given the litigious environment in the city where this blasting occurred.

REFERENCES

Abeel, P A, 2012. Building and Crack Response to Blasting, Construction Vibrations and Weather Effects, Mater of Science thesis, Department of Civil & Environmental Engineering, Northwestern University, Evanston, IL, USA.

Dowding, C H, 1996. *Construction Vibrations* (Prentice Hall: Saddle River, NJ, USA).

Hamdi, E, 2015. Report of Fulbright Study of the Response of Urban Structures to Ultra High Frequency Excitation, Internal Report, Department of Civil and Environmental Engineering, Northwestern University, Evanston, IL, USA.

Turnbull, R, 2012. Personal Communication (InstanTEL: Ottawa, Canada).

Siskind, D E, Stagg, M S, Kopp, J W, and Dowding, C H, 1980. RI8507 - Structure Response and Damage Produced by Ground Vibration from Surface Mine Blasting. (U. S. Bureau of Mines, Washington, DC, USA).

Wheeler, R, 2012. Personal Communication, White Seismograph (Joplin, MO, USA)

FIGURES

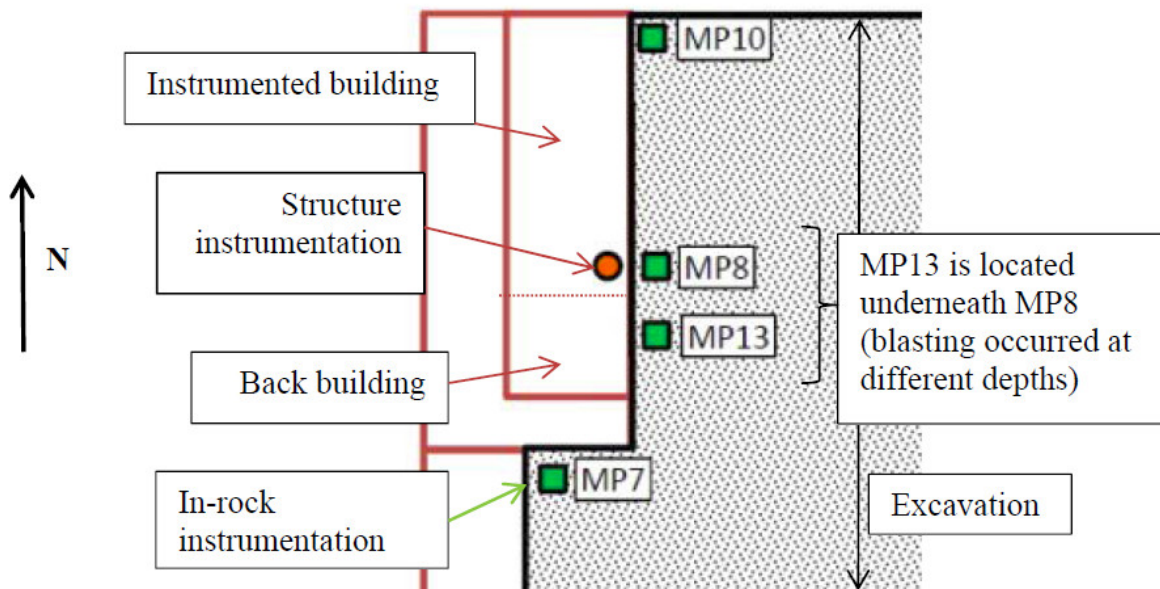
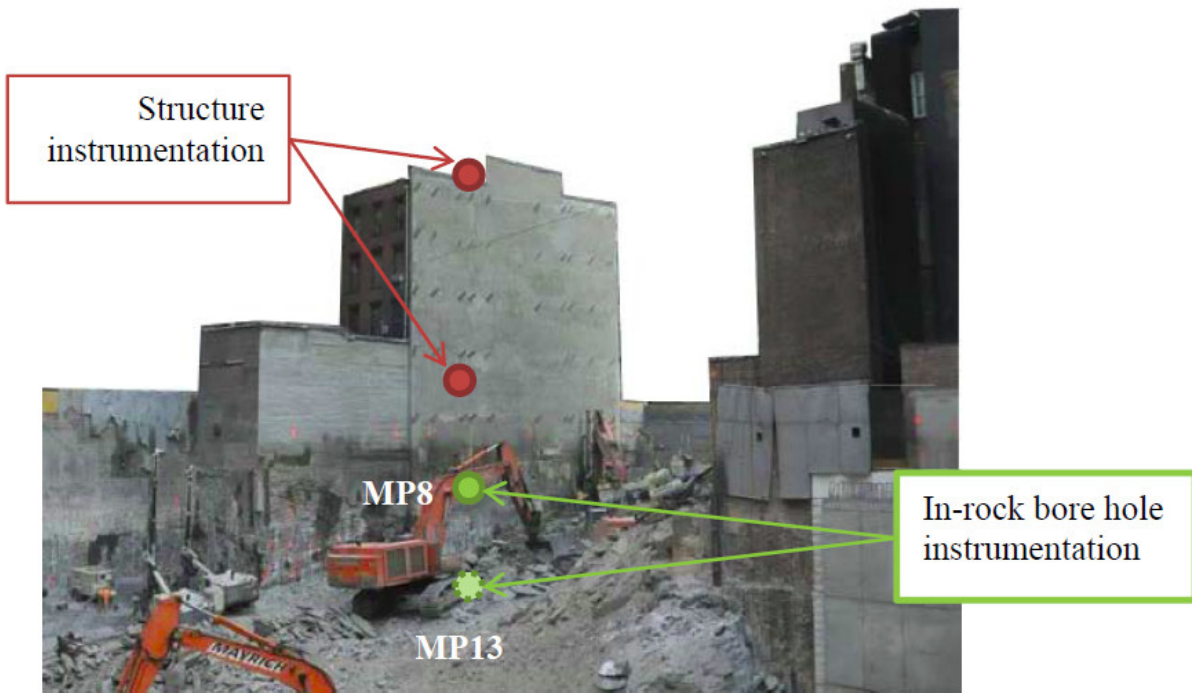


FIG 1 – Geometry of the site with a) Elevation photograph of instrumented structure showing locations of the velocity geophones on the structure; top and b) plan view of the excavation (stippled) with the structure and locations of velocity geophones in the rock.

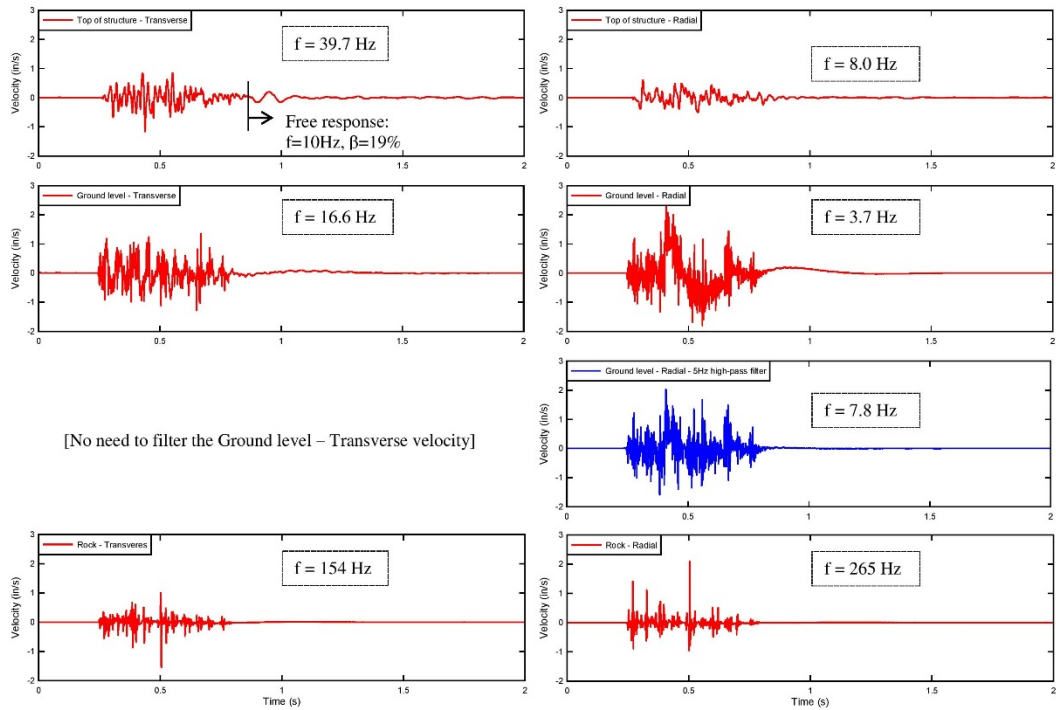


FIG 2 – Time histories of the excitation transverse (left) and radial (right) rock – excitation (bottom) and ground (middle) and top (top) response motions that show the declination of dominant frequency from excitation and time delay between rock and top motions (relative to vertical line).

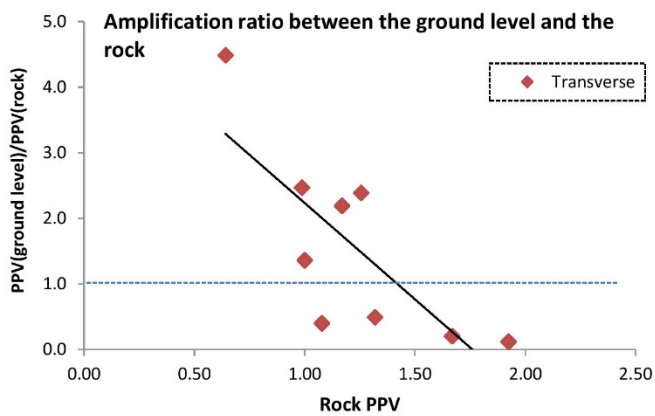
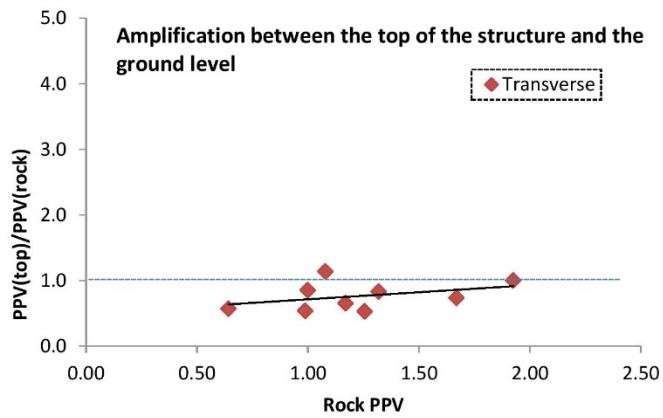
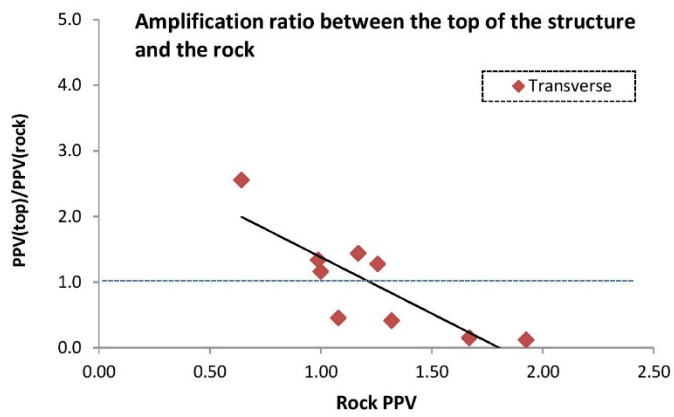


FIG 3 – Comparison of ratios of transverse peak particle velocities (PPVs) with PPV in the rock shows deamplification rather than amplification: top –top/rock; middle – top/ground level; bottom – ground/rock (Rock PPV's are ips where 1 ips = 25.4 mm/s)

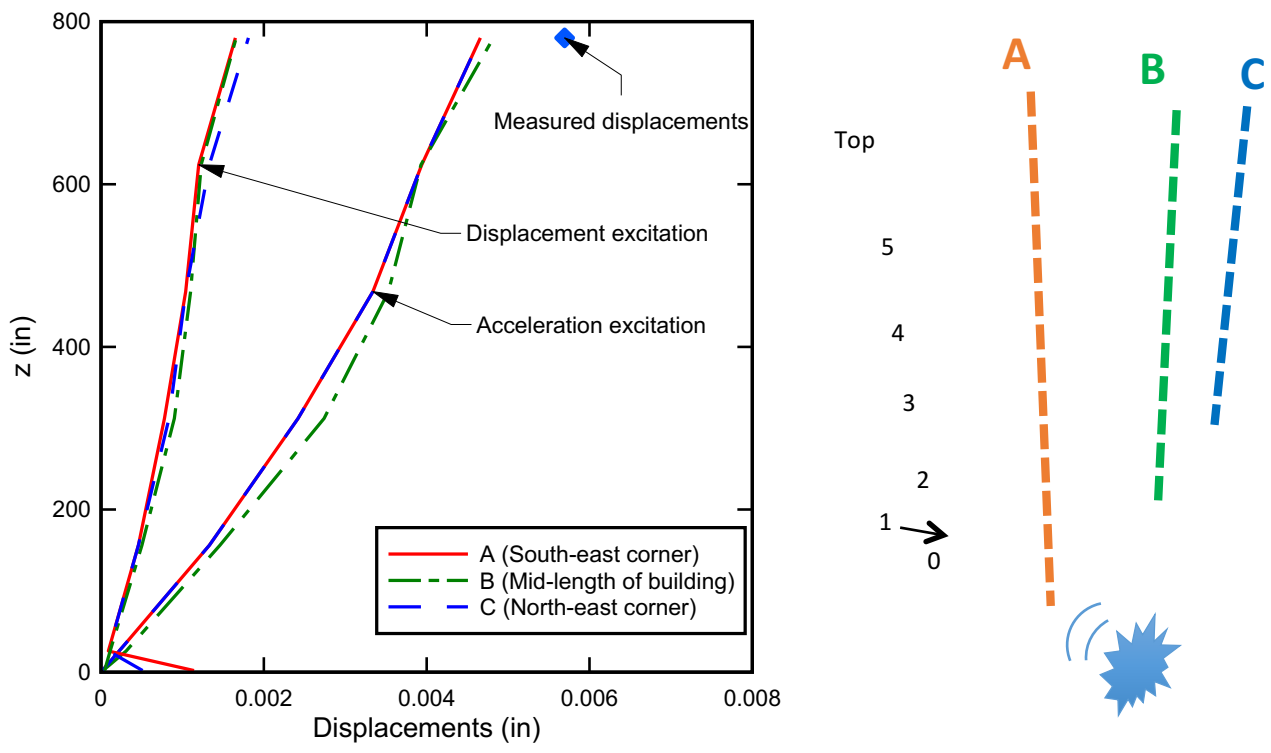


FIG 4 - 3D building model (right) showing location of the blast and locations for comparison of measured and calculated displacements and model response (left) showing: relative displacements calculated with 3D model (lines) and measured integration of top velocity time history (1 in = 25.4 mm)

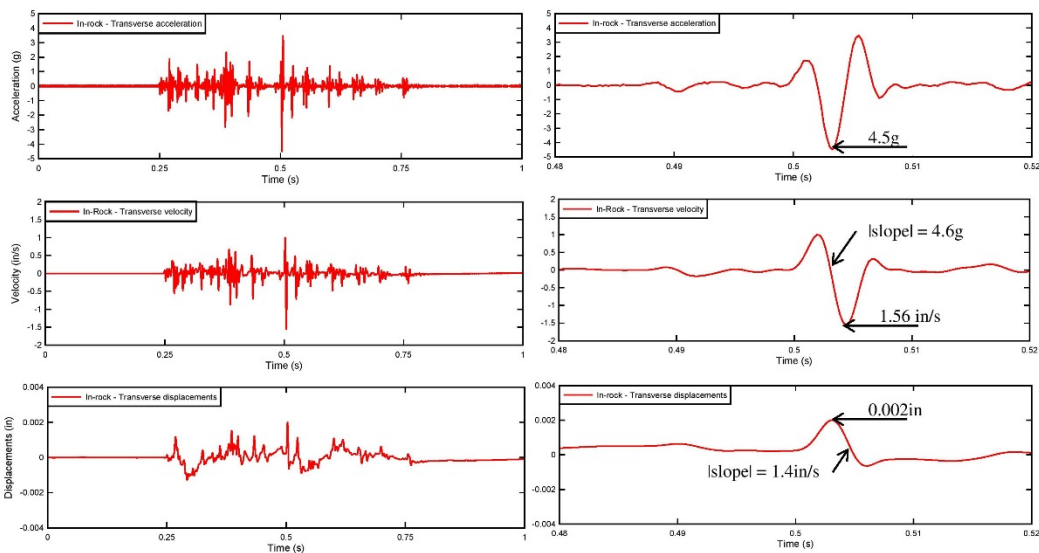


FIG 5 - Time histories of excitation motions employed for various modeled inputs (left):(top) acceleration (middle) velocity and (bottom) displacement compared (right) to the peaks of the dominant pulse (1 in = 25.4 mm)

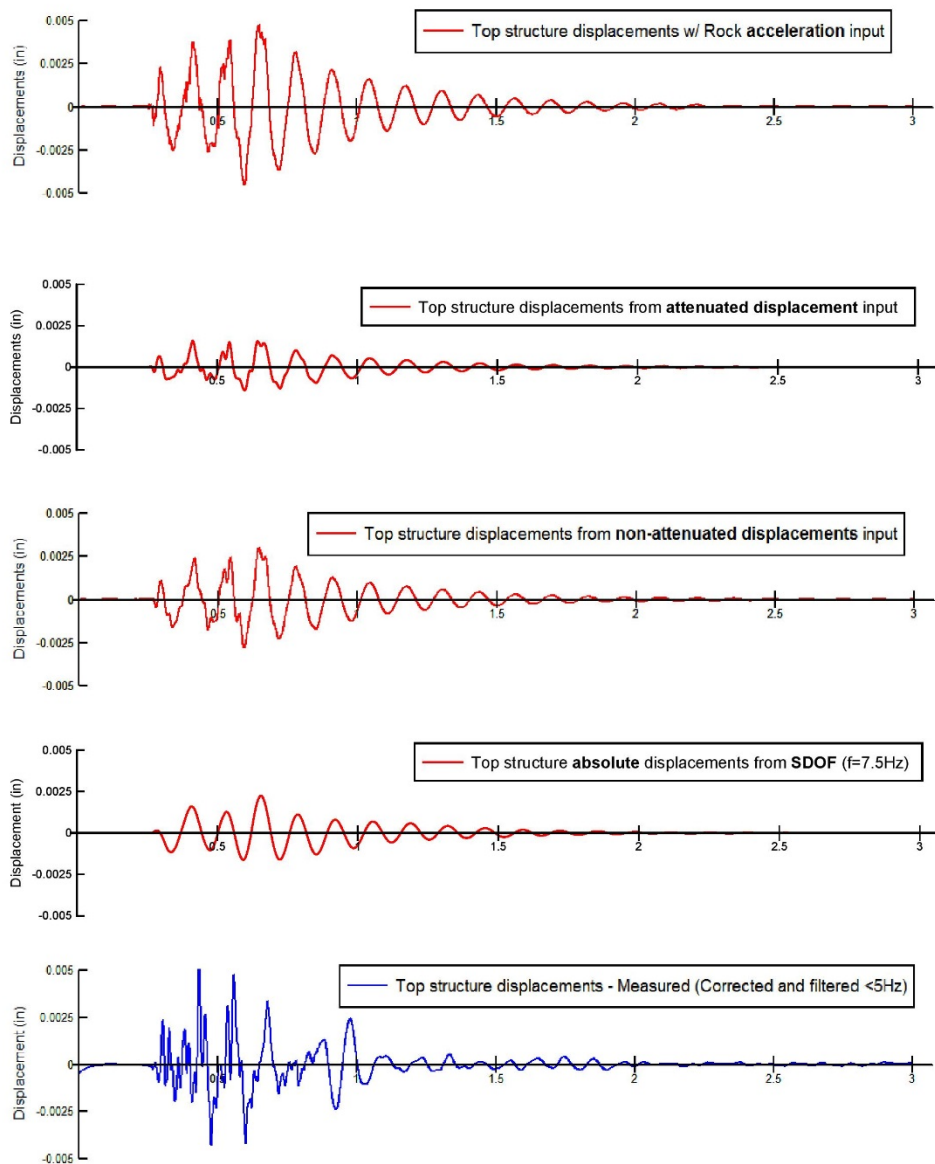


FIG 6 - Comparison of modelled/simulated (top 4 time histories) and measured (bottom) displacements at the top of the structure. Acceleration (top) was applied uniformly to structure. Attenuated displacement was delayed along base by the propagation velocity. SDOF and non-attenuated displacements were uniformly applied to the respective models (1 in = 25.4 mm).

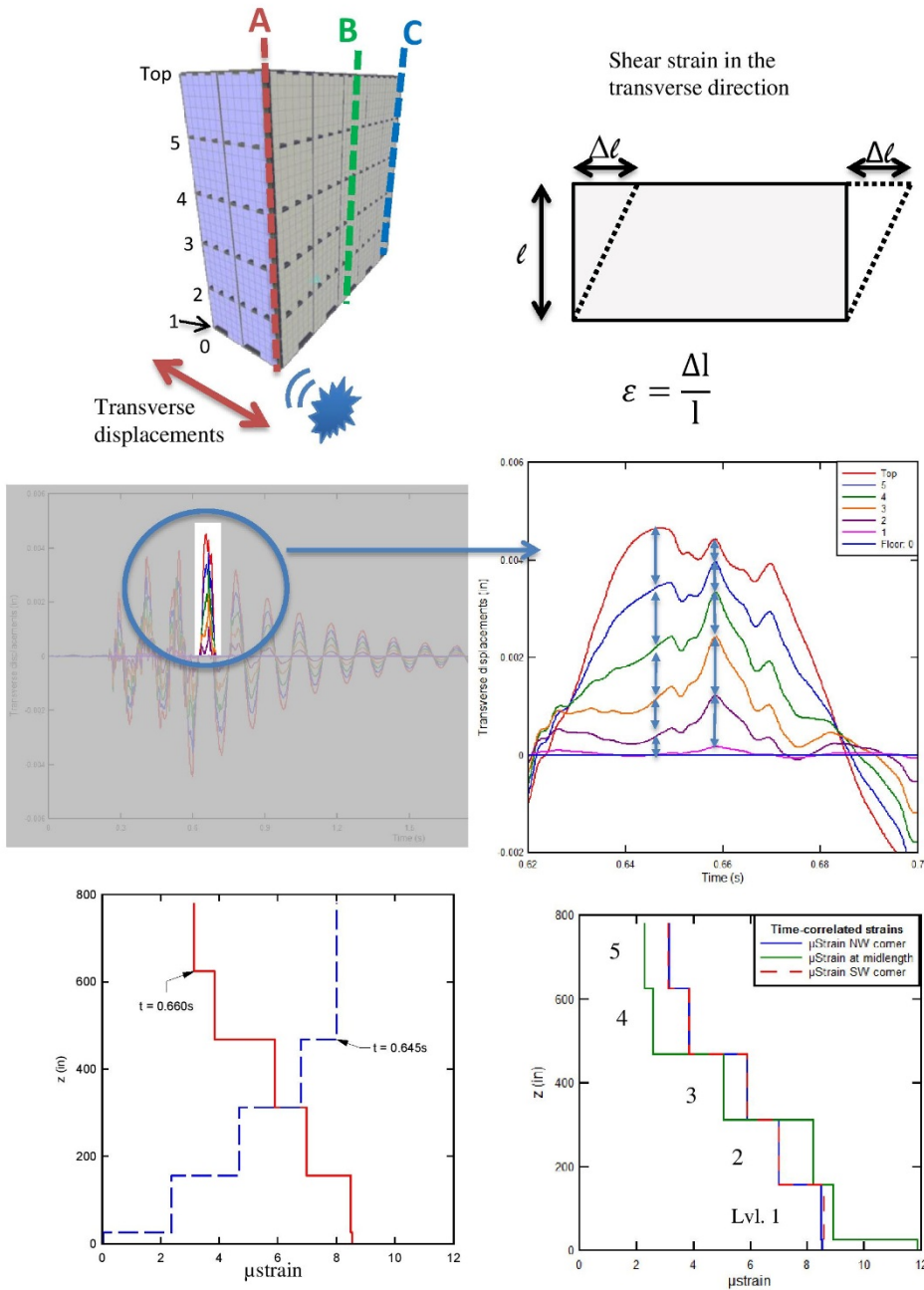


FIG 7 - Procedure for calculating transverse shear wall strains from global differential displacement (top). 3D model results (middle) showing progression of strain location with time along A. Variation of model strains at differing times showing concentration of model strains at the bottom (1 in = 25.4 mm/s).

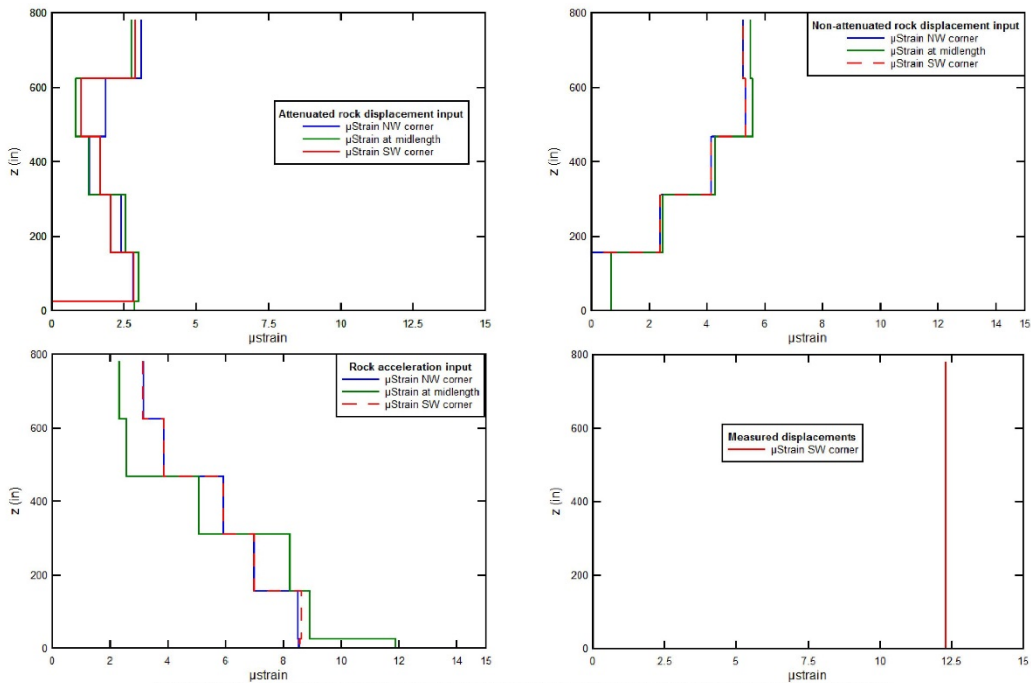
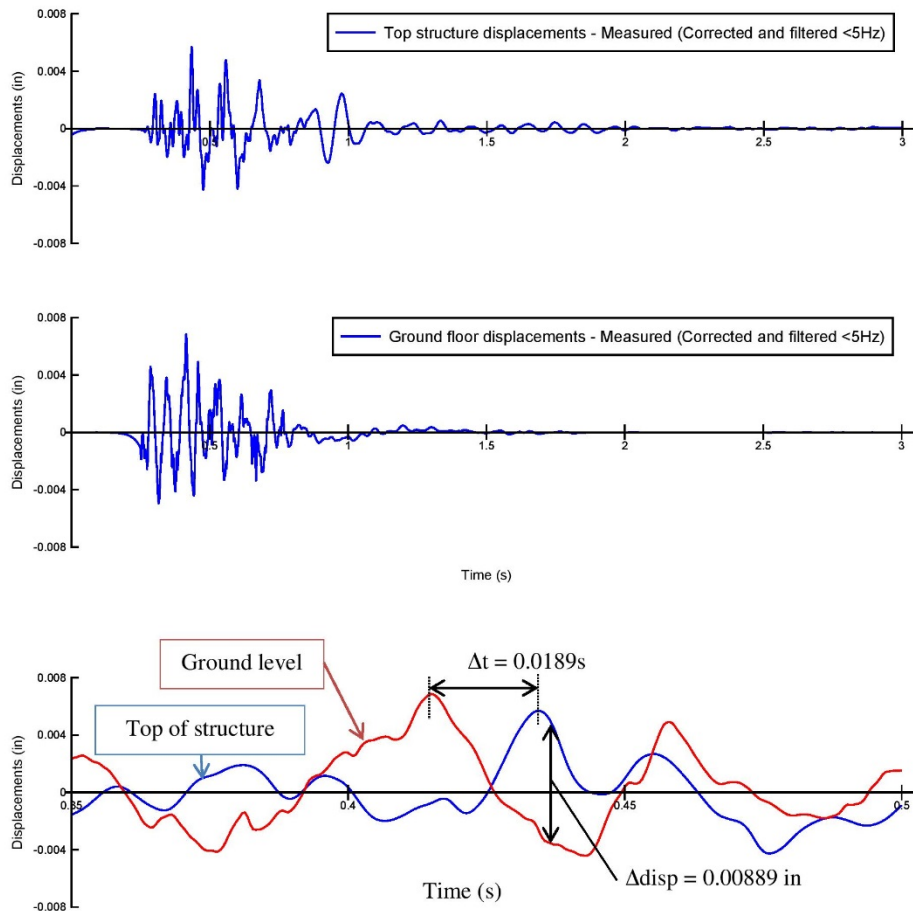


FIG 8 - Comparison of the 3D model inter-story shear strains calculated with various input motions compared with those calculated (“measured”) from the difference in top and bottom displacements (bottom right). Differences in the distribution of strains with elevation for the single acceleration and single displacement time history point out the challenges in model simulation (1 in = 25.4 mm/s).



Global shear strain calculation:

$$\Delta d = \text{Maximum differential displacement} = 0.00889 \text{ in}$$

$$\epsilon = \text{Global shear strain} = \frac{\Delta d}{\Delta H} = \frac{0.00889 \text{ in}}{780 \text{ in}}$$

$$\epsilon = 11.4 \times 10^{-6} = \underline{11.4 \mu\text{strains}}$$

Propagation delay:

$$\Delta t = 0.0189 \text{ s}$$

$$\Delta H = 780 \text{ in} = 65 \text{ ft} = 19.8 \text{ m}$$

$$C_c = \frac{65 \text{ ft}}{0.0189 \text{ s}} = \underline{3440 \text{ ft/s}} = 1049 \text{ m/s}$$

FIG 9 - Example calculation of global shear strain from the difference between time correlated displacement time histories showing the wave propagation difference in the arrival of the peak at the top and bottom of the structure. The difference in arrival times can then be employed to calculate the propagation velocity within the structure (1 in = 25.4 mm/s).

TABLES

TABLE 1

Summary of Measured Peak Particle Velocities (PPV) in inches/sec (1 in/s = 25.4 mm/s) and the Ratio between Response (structure) and Excitation (rock).

In-rock measurement location		MP8		MP10						
MAX PPVs (principal pulse)		Event #1	2	3	4	5	6	7	8	9
Structure	Radial Top	0.61	0.88	0.71	0.81	0.24	0.3	0.74	0.13	0.13
	Radial Ground floor	2.6	3.24	2.36	3.2	0.72	0.85	3.72	0.64	0.59
	Transverse Top	1.16	1.32	1.64	1.68	0.49	0.54	1.6	0.25	0.23
	Transverse Ground floor	1.36	2.44	2.88	2.56	0.43	0.65	3	0.34	0.23
Rock	Radial	2.09	1.11	2.13	2.26	1.87	2.07	2.44	1.30	0.75
	Transverse	1.00	0.99	0.64	1.17	1.08	1.32	1.26	1.67	1.93
RATIOS	PPVtop/PPVgroundfloor									
	Radial	0.23	0.27	0.30	0.25	0.33	0.35	0.20	0.20	0.22
	Transverse	0.85	0.54	0.57	0.66	1.14	0.83	0.53	0.74	1.00
	PPVtop/PPVrock									
	Radial	0.3	0.8	0.3	0.4	0.1	0.1	0.3	0.1	0.2
	Transverse	1.2	1.3	2.6	1.4	0.5	0.4	1.3	0.1	0.1
PPVgroundfloor/PPVrock										
Radial	1.2	2.9	1.1	1.4	0.4	0.4	1.5	0.5	0.8	
Transverse	1.4	2.5	4.5	2.2	0.4	0.5	2.4	0.2	0.1	

TABLE 2

Parameters Employed in the Development of the 3D SAP 2000 Model.

Parameter	Value
Building	
Width	9.55 m (376 in)
Length	19.81 m (780 in)
Height	19.51 m (768 in)
Material	
Unit weight	2002 kg/m ³ (125 pcf)
Compressive strength f _c	27.58 MPa (4000 psi)
Modulus E	2482 MPa (3.6x10 ⁵ psi)
Poisson's Ratio U	0.2
Frame dimensions	
Beams (thickness x width)	0.2 x 0.3 m (8 x 12 in)
Columns (width x width)	0.3 x 0.3 m (12 x 12 in)
Material damping	5%
Slabs thickness	0.2 m (8 in)
Walls thickness	0.36 m (14 in)
Bay dimensions	3.51 x 3.91 x 3.96 m (138 x 154 x 156 in)
Number of bays	50

TABLE 3

Time Delays and Attenuations Employed in Perturbing the Model with Variable Displacements (1 in = 25.4 mm).

Column #	x (in)	y (in)	Distance from blast (in)	Propagation velocity (ft/s)	Delay (ms)	Amplitude (%)
1	0	0	0		0.00	100
2	138	0	138		1.28	79
3	276	0	276		2.56	63
4	0	154	154		1.43	79
5	138	154	206.8		1.91	72
6	276	154	316.1		2.93	60
7	0	308	308		2.85	63
8	138	308	337.5		3.13	59
9	276	308	413.6	9,000	3.83	52
10	0	462	462		4.28	50
11	138	462	482.2		4.46	48
12	276	462	538.2		4.98	43
13	0	616	616		5.70	39
14	138	616	631.3		5.85	38
15	276	616	675		6.25	35
16	0	770	770		7.13	31
17	138	770	782.3		7.24	30
18	276	770	818		7.57	28